Acta Physica Hungarica 55 (1—4), pp. 489—500 (1984)

SIMPLE MODELS FOR ALMOST CENTRAL ASYMMETRIC HEAVY-ION COLLISIONS AT MODERATE ENERGIES*

L. P. CSERNAI

School of Physics and Astronomy, University of Minnesota
Minneapolis, MN 55455, USA
Central Research Institute for Physics,
1525 Budapest, Hungary

and

G. FÁI

Smith Laboratory of Physics, Kent State University, Kent, OH 44242, USA
Institute for Theoretical Physics, Roland Eötvös University, 1088 Budapest, Hungary

One-dimensional hydrodynamical model is applied to almost central asymmetric heavy ion collisions in the energy range 50—500 MeV/nucleon. Cross sections and rapidity distributions are evaluted and compared to experiments. The time development of the density profiles as well as the properties of the heavy target residues are investigated. The number of participant and spectator nucleons is estimated on the basis of the model.

1. Introduction

In recent years two energy regions were studied extensively in heavy-ion physics. Projectiles up to the energy of 5—10 MeV/nucleon were produced by conventional accelerators while in Berkeley and Dubna the GeV region was investigated. Between these two energy regions an extremely interesting area is now under experimental investigation at CERN.

Around projectile energies of 20—50 MeV/nucleon we may switch from the quantummechanical description to classical hydrodynamics and up to 100 MeV/nucleon both approaches yield similar results [1, 2]. At beam energies from 100 to 500 MeV/nucleon the hydrodynamical approach seems to be rather good [3, 4]. At higher energies the basic conditions for the applicability of hydrodynamics are less obviously fulfilled and in the GeV region the usual one-fluid hydrodynamical approach can be justified only if unusual processes (pion condensation or transition to quark phase) enhance the local equilibration [5] sufficiently.

* Dedicated to Prof. I. Kovács on his 70th birthday

Thus, in this unexplored energy region collective (hydrodynamical) nuclear motions play an essential role while at lower energies usual quantum mechanics and at very high energies simultaneous single particle collisions are conspicuous.

The energy region 50—500 MeV/nucleon is very rich not only in phenomena but also in fundamental physics. The appearance of pion condensation was expected in this energy region and other unusual forms of nuclear matter are likely to show up.

In the present work we discuss only the asymmetric collisions with not too high impact parameters $b < R_t - R_p$. A qualitative description of these processes was given recently by Bondorf [6]. In Sections 2 and 3 the formation and evolution of the "hot spot" is described in the one-dimensional hydrodynamical model (introduced in [4] and [7]) for central collisions. In Section 4 a simple schematic model is given for asymmetric central collisions in terms of a hot spot. In Section 5 we give a summary and discussion.

2. One-dimensional hydrodynamical model

In the present work we use the viscous, relativistic one-dimensional model first described in [7]. (More details can be found in [4]). The one-dimensional model yields only a rough description of a central asymmetric collision where the impinging projectile produces a dense "hot spot" and this "hot spot" expands in transversal directions while penetrating the target. Assuming that the transversal expansion is uniform and not much more rapid than the penetration the particles involved in the process are inside a cone of angle Φ. Depending on the value of Φ a different number of nucleons from the target belongs to the spectators and to the participants, respectively (Fig. 1). In our model only the participants are involved in the hydrodynamical flow. The radius of the hypothetical tube, where the one-dimensional collision takes place, is determined in such a way that the intersection of the target and this cylinder produces the proper number of spectators (Fig. 2):

$$\bar{R}(\Phi) = R_t \sqrt{1 - \frac{A_{sp}(\Phi)^{2/3}}{A_t}} . \tag{1}$$

The spectators are obviously not absolutely undisturbed, but we can take their excitation as a secondary effect. A rough approximation of the expansion angle Φ can be given by the comparison of the sound and shock front velocities:

$$\Phi = \operatorname{arctg}\left[\frac{v_{\text{sound}}}{v_{\text{shock}}}\right] \approx 10°—20°. \tag{2}$$

The expansion angle decreases for higher beam energies and for "harder" equations of state because both effects increase the velocity of the shock front.

In the asymmetric case the propagation of the compression shock is not stationary (Fig. 3). The one-dimensional model yields an upper bound for the

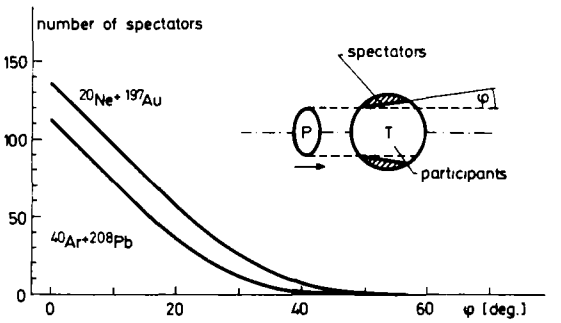

Fig. 1. Number of spectator nucleons as function of the expansion angle Φ for the reactions discussed in the text. The definition of Φ is represented on the attached scheme

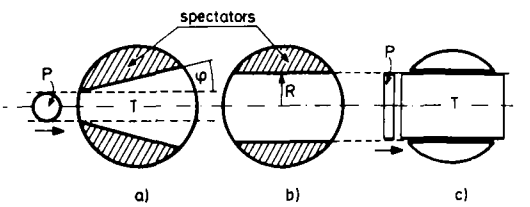

Fig. 2. Schematic representation of the introduction of the one-dimensional model. The radius of the "reaction tube" $\bar{R}$ is uniquely defined as a function of Φ, A_p and A_t by the prescription that the number of spectators in (a) and (b) should be equal. In the hydrodynamical flow the slabs of projectile and target participants are involved while the spectators are considered only after the "break-up" (c)

penetration depth of the "hot spot" into the target. As we can see in Fig. 3 the velocity of the shock front decreases and its width increases as time proceeds. The reason for this basically lies in the asymmetry: behind the shock front, after the full compression of the projectile at ≈ 3 fm/c, an expansion starts to pull the nucleons back, thereby attracting the compressed region in backward directions.

In all investigated cases the shock wave penetrated the whole target but in most cases the density increase of the shock was much less when the shock wave reached the back surface of the target, than the initial density increase. In Fig. 3 we can see that the contour of the maximum density ($n > 2n_0$) ends already at 20 fm/c, while the shock front reaches the back surface of the target at ≈ 24 fm/c. The largest amount of nuclear matter with maximum density can be observed always at the full compression of the projectile (i.e. immediately before the last cell of the projectile turns back at t_{comp} (Fig. 4). Up to this time the shock fronts propagate symmetrically into the target and projectile in the mean velocity system. This propagation is close to stationary and so the velocity of the shock can be obtained from the Rankine—Hugoniot equations [4]. After t_{comp} the free end of the projectile begins to expand and later it explodes (at the break-up) while on the target side the shock front propagates further. However, its propagation after t_{comp} is already not stationary and the shock cannot be described by

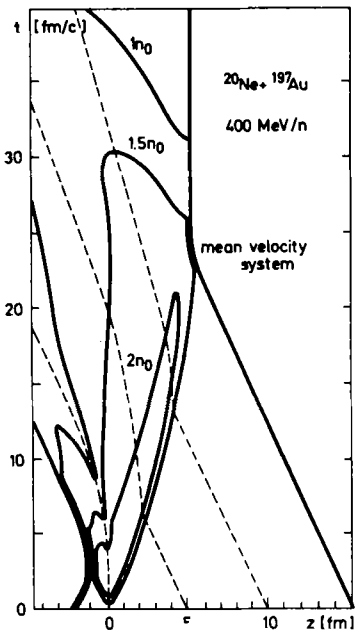

Fig. 3. Hydrodynamical model calculation for the reaction $^{20}Ne+^{197}Au$ at a beam energy 400 MeV/nucleon. The space-time development of the density distribution in one spatial dimension along the z-axis is shown. Full curves represent contours of the density distribution. At a fixed time (e.g. 5 fm/c) the actual density profile can be read from a cut parallel to the z-axis (e.g. for the moment given above a density $n \geq 2n_0$ is reached for 0.5 fm $\leq z \leq$ 2 fm). Dashed curves represent the world lines of individual fluid elements (i.e. the motion of nucleons in space-time). The equation of state of [3] has been used with $n_0 = 0.145$ fm^{-3}

the Rankine—Hugoniot relations. The amount of matter with maximum compression is decreasing after t_{comp} and at the time $t_{1/2}$ it falls to the half of its maximum value. In Fig. 4 the definitions of the different times and lengths are shown. The stationarity of the shock can be studied (Fig. 5) by the comparison of the average shock velocities relative to the projectile and target (L_p/t_{comp} and L_T/t_{eff}, respectively). It is also interesting to study the position of $t_{1/2}$ that shows the lifetime of the compressed matter.

In Fig. 5 the results of two reaction calculations are summarized. According to our model the results depend on the angle Φ (or on the number of spectators). For both reactions the shock is not stationary in the target where its average velocity L_T/t_{eff} is less than that in the projectile (L_p/t_{comp}). The difference is increasing when the angle is increased.

The position of the time $t_{1/2}$ is even more sensitive to the angle Φ. We have to remember the definitions of the times t_{comp} and $t_{1/2}$ (Fig. 4): the amount of dense matter is increasing from zero to its maximum value (at t_{comp}) and then decreasing to half of its amount (at $t_{1/2}$). So the quantity $l_{comp}/(t_{1/2} - t_{comp})$ characterizes the "boiling speed" of the hot spot. For both reactions shown in Fig. 5 we can see that this speed has its

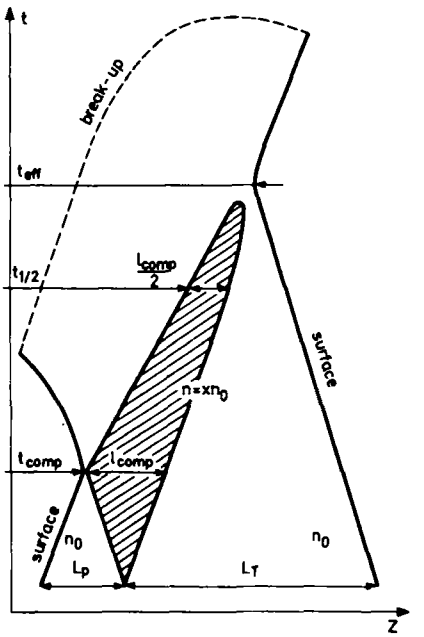

Fig. 4. Schematic representation of the density contour plot of an asymmetric collision in two dimensional space-time for the definition of the characteristic times and lengths of the process. All quantities are measured in the mean velocity system where the projectile and the target approach each other with the same speed. The parameter x defines the contour of the maximum density region (hot spot)

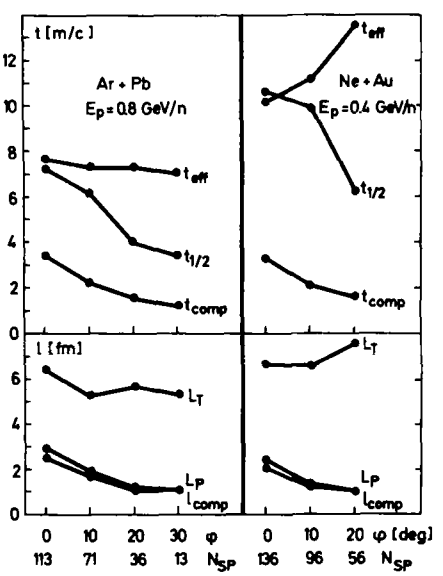

Fig. 5. Dependence of the characteristic times and lengths on the expansion angle Φ for the reactions Ar + Pb (0.8 GeV/nucleon) and Ne + Au (0.4 GeV/nucleon). The high density regions are taken above $n = 2.5\, n_0$ and $n = 2n_0$ respectively

maximum at $\Phi = 0°$, then drops sharply to the 1/3 of the maximum at $\Phi = 10°$ and it is slowly increasing for larger angles. The reason for this unexpected behaviour is the following: at $\Phi = 0°$ the shock front reaches the back surface of the target quicker than the boiling or expansion from the projectile side could decrease the maximum density reached in the shock (Fig. 6) so the expansion into the direction of the target will be more rapid due to the higher gradient. For the larger Φ-angles the length of the compressed matter (l_{comp}) is shorter and the expansion wave from the projectile side reaches the shock front earlier than this latter arrives to the back surface of the target. Thus the boiling of the dense hot spot is allowed into one direction only and therefore it is slower. From the target side the shock front is exposed to a constant flux of incoming nuclear matter and when the maximum density of the shock is decreased already (from the projectile side) the constant incoming flux yields a shock of decreasing velocity.

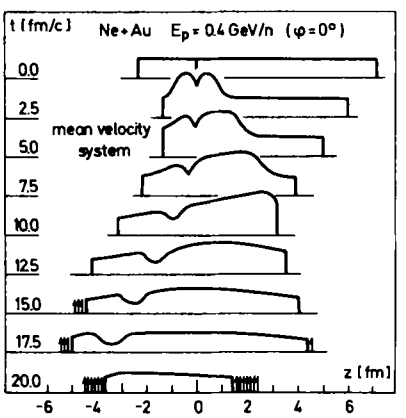

Fig. 6. Time dependence of the density profiles. At $t = 0$ fm/c the fluid consists of two slabs of normal nuclear density. Later a central decrease develops due to the initial condition and a higher central temperature ensures the equilibrium of pressure. This deviation in the centre does not disappear because the heat conduction is neglected in the model. The arrows represent the fluid cells which broke up within the last time interval

3. Spectrum of the emitted nucleons in the hydrodynamical model

In the hydrodynamical flow a dilute stage of matter can be reached when the interactions cannot ensure equilibrium any more. At this moment our description is changed from hydrodynamics to the free relativistic Fermi—Dirac statistics. The details of this "break-up" process are described in [4]. However, in the present model spectators should also be considered. Spectators are described by the same relativistic Fermi—Dirac distribution as participants and we assume that their average thermal excitation is $T_s = 6$ MeV. This excitation comes from the relatively large surface energy of the spectators that fill volumes of strange shape.

In Fig. 7 the double differential cross section of the reaction Ne+Au at 0.4 GeV/nucleon is shown. One can distinguish the contribution of the low temperature spectators (the peak around 10—15 MeV) and that of the participants This structure is observed in the experiments of Gutbrod et al [8], where high multiplicity events were selected. At 90° the hydrodynamical model gives lower cross sections than the experimentally observed ones. This difference can be explained by the one dimensional nature of our model (transversal hydrodynamical flow is not possible). The energy independence of the forward angle cross sections observed between 40 and 100 MeV is caused by the broad peak of the cross section. At higher energies the cross sections show the usual decrease (Fig. 8).

The separation of target spectators is possible in the high multiplicity events and here projectile spectators are not expected. In an experiment of higher energy [9] the contribution of the spectators can be discriminated from the contribution of participants. Our model calculations produced a sharp increase below 50 MeV for the invariant cross section of 800 MeV/nucleon Ar+Pb collision. In the experiment [9] this low energy region is not investigated in detail so in the experimental cross section the low energy peak of spectators was not observed. However, on the rapidity spectrum the distinction is more convenient and both target and projectile spectators were observed in the experiment [9]. Projectile spectators do not occur in almost central collisions, so the selection of high multiplicity events would eliminate the low energy peak in the rapidity plot around y_{proj}. Our calculations for the same central collisions produced similar results (Fig. 9). The contribution of projectile spectators is obviously

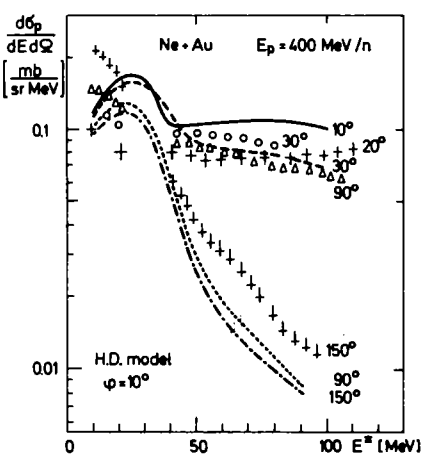

Fig. 7. Double differential proton cross section of central Ne+Au collision at 0.4 GeV/nucleon (in the lab. system). Full, dashed, dotted and dashed-dotted curves are obtained in the present calculation. Experimental points of Gutbrod et al are taken from [8], and for their normalization an approximate cross section $\sigma_0 \approx 17$ mb was used. The low energy peak in the forward angle calculated cross sections is produced by the spectators of temperature 6 MeV. Similar enhancement in the experimental cross sections at lower energy is probably of the same origin

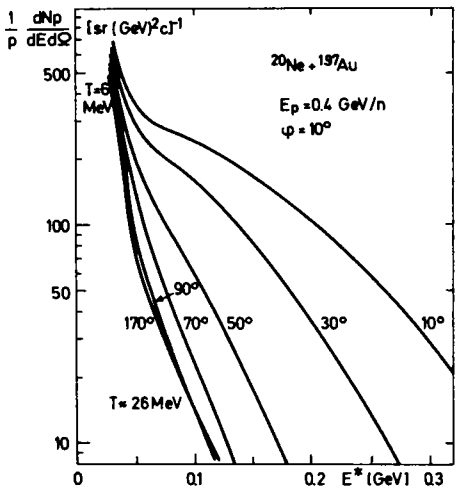

Fig. 8. Invariant proton cross section of the central Ne+Au 0.4 GeV/nucleon collision obtained in the present hydrodynamical model. In transverse directions the low temperature target spectator contribution can be distinguished from the higher break-up-temperature (≈ 26 MeV) participants. In forward angles the cross section is not exponential due to the flow

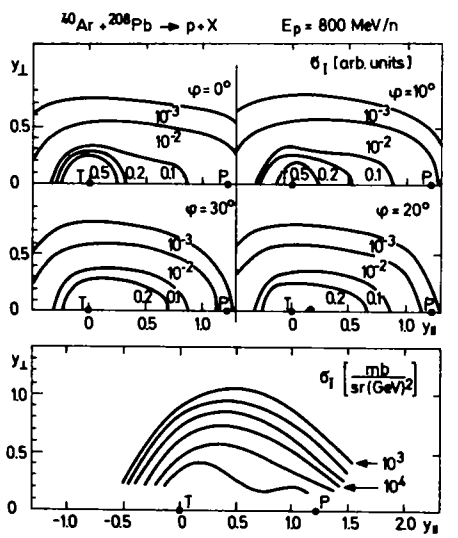

Fig. 9. Rapidity contour plots of the invariant proton cross section for central Ar + Pb collision obtained in the present model for different expansion angles Φ, together with the experimental invariant cross section for the same reaction [9]. (It should be noted that in the experiment [9] there was no selection for high multiplicity events). Observe that the experimental rapidity distribution of target spectator peaks displaced from $y = 0$ due to the target recoil. This effect will be treated only in the subsequent phenomenological model

absent in the calculated spectra and comparison with experiments shows that the angles around $\Phi = 10°—20°$ are the most realistic ones for the description of almost central asymmetric heavy ion collisions.

4. Phenomenological model

In this Section we present a phenomenological model for almost central asymmetric heavy ion collisions at moderate energies. The model is capable of calculating the recoil properties of the target residue.

We assume that the process of the asymmetric heavy ion collision (Fig. 1) can be described in two stages: i) at the first impact a region of the target and the projectile is equilibrated and moves with a "hot spot velocity" $\mathbf{v}_h$ and ii) nucleons emerge from the equilibrated region with an isotropic momentum distribution; some of them get absorbed in the target residue, which in this way acquires a recoil momentum. (This absorption shadow is neglected in the hydrodynamic model presented in Section 2).

We have one free parameter, the number of nucleons a, participating in the hot spot from the target. (The connection of a and the quantities, defined in Figs 2 and 4 will be discussed later). In the almost central reactions considered all A_p nucleons of the projectile clearly participate in the hot spot. To describe the first stage of the reaction we use energy and momentum conservation. (The calculations in this Section were carried out in the laboratory system for convenience). Assuming that the total available energy goes into the kinetic energy of the ordered motion of the hot spot with the collective velocity $\mathbf{v}_h$ and into the kinetic energy of the Fermi gas, we get for the average statistical velocity

$$\bar{v}^2 = \frac{A_p a}{(A_p + a)^2} v_0^2, \tag{3}$$

where $v_0 = \sqrt{\frac{2E_{\mathrm{LAB}}}{m_N A_p}}$ is the beam velocity.

In the present model we use a further simplifying assumption: we consider $\bar{v}^2$ to be the average corresponding to a sharp Fermi sphere. While this is certainly not the case in the hot spot, the sharp Fermi sphere allows us to define a Fermi speed v_F, which, as we shall see, proves to be extremely useful in our first, unsophisticated estimates. This approximation is sufficient for our qualitative purposes.

Using $\bar{v}^n = \frac{3}{n+3} v_F^n$ from [10] one gets

$$v_F = \sqrt{\frac{5}{3} \frac{A_p a}{(A_p + a)^2}}\, v_0, \tag{4}$$

where the factor $\frac{5}{3}$ is a consequence of the sharp Fermi distribution and should not be taken seriously.

Now, in the second stage of the reaction we have a hot spot moving still inwards to the target with the velocity $\mathbf{v}_h$. This hot spot will be represented by a Fermi sphere of radius v_F, displaced with $\mathbf{v}_h$ in velocity space (Fig. 10). In other words we have the same picture as in Section 3 up to the time t_{comp} (Fig. 4), but in our simple schematic model the development after t_{comp} is described by the single-particle decay of the hot spot. All those particles of the hot spot which have a velocity component facing the target ($v_x > 0$) are assumed to be absorbed in the residue (Fig. 10).

The fraction f of the hot spot nucleons absorbed in the target residue is defined by

$$f = \frac{\text{volume absorbed}}{\text{volume of Fermi sphere}} = \frac{\int\limits_{v_x>0} d\tau}{\int\limits_{\text{sphere}} d\tau}, \tag{5}$$

where the integration goes over the hot spot velocities. We get for the mass number of the target residue

$$A_{tr} = A_t - a + f(A_p + a). \tag{6}$$

It is straightforward to calculate the recoil velocity of the target: first we calculate the average velocity $\mathbf{V}$ of the absorbed hot spot particles by the prescription

$$\mathbf{V} \int\limits_{v_x>0} d\tau = \int\limits_{v_x>0} \mathbf{v} d\tau \tag{7}$$

and get the recoil velocity $\mathbf{v}_r$ from

$$f(A_p + a)\mathbf{V} = A_{tr}\mathbf{v}_r. \tag{8}$$

In Fig. 11 the recoil velocity is plotted as a function of a for the reaction $^{12}C + ^{208}Pb$ at the energy $E_{LAB} = 86$ MeV/nucleon. It can be seen that the recoil velocity is a slowly increasing function of the number of target participants, a, for $12 < a < 50$. (The upper limit on a comes from the requirement that the excitation energy in the hot spot should

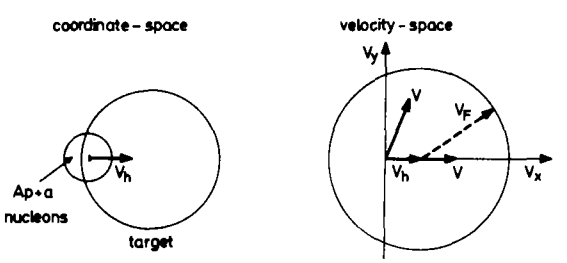

Fig. 10. The representation of the hot spot in the phenomenological model, both in coordinate and velocity space

be at least above the binding energy in order to make the concept of hot spot sensible. On the other hand at the time $t=t_{comp}$, $a=A_p$ according to the principle of equal participation [6] and at a time $t_{comp}<t<t_{1/2}$, $a>A_p$.).

From Fig. 3 we can get an estimate of a. Assuming that the first stage of the reaction (the local equilibration of the hot spot) is completed at $t\approx 2t_{comp}$ and comparing the length of the unshocked region at this particular instance of time to the original length of the target L_T, we arrive at a very rough guess on what a could be. An inspection of Fig. 3 suggests that a is at around the upper end of the interval displayed in Fig. 11. This means a recoil velocity $v_r\approx 0.045$ c. It should be noted, however, that this recoil was obtained under the assumption of total absorption in the target residue. Taking into account the transparency of the target material may reduce the above value of v_r considerably.

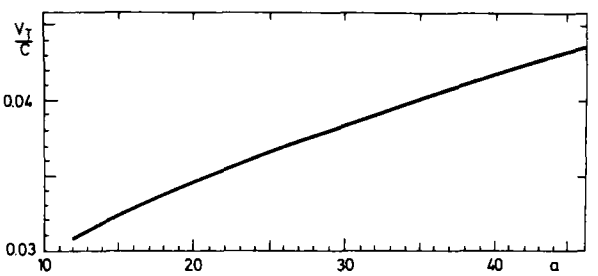

Fig. 11. The recoil velocity of the central $^{12}C+^{208}Pb$ reaction at 86 MeV/nucleon beam energy as a function of the number of participants a of the hot spot from the target

5. Summary

We presented two models for the description of almost central asymmetric heavy ion collisions at moderate energies. The hydrodynamical model gave results which compare with the experimental values rather well, but suffer from the onedimensionality of the present description. In the framework of the phenomenological model we predicted recoil properties of the target-residue.

Finally we emphasize that the one dimensional hydrodynamical model seems to favour an opening angle (Fig. 1) $\Phi\approx 10°$ at these energies. It is also possible to get an estimate from the hydrodynamical model for the free parameter of the phenomenological model. This suggests that the number of participants a of the hot spot from the target (Fig. 10) is around $a\approx 0.35A_t$ in the reaction $^{20}Ne+^{197}Au$ at the energy 400 MeV/nucleon.

References

1. C. Y. Wong, J. A. Maruhn and T. A. Welton, Phys. Lett., *66B*, 19, 1977.
2. H. Stöcker, R. Y. Cusson, J. A. Maruhn and W. Greiner, Z. Phys., *A294*, 125, 1980; Phys. Lett., *44*, 725, 1980.
3. A. A. Amsden, F. H. Harlow and J. R. Nix, Phys. Rev., *C15*, 2059, 1977; J. R. Nix, Prog. Part. Nucl. Phys., *2*, 237, 1979; J. I. Kapusta and D. Strottman, Phys. Rev., *C23*, 1282, 1981.
4. L. P. Csernai and B. Lukács, Central Research Institute for Physics, Budapest Report (1979), KFKI-79-58; L. P. Csernai and H. W. Barz, Z. Phys., *A296*, 173, 1980 and L. P. Csernai, B. Lukács and J. Zimányi, Nuovo Cim. Lett., *27*, 111, 1980.
5. M. Gyulassy and W. Greiner, Ann. Phys., *109*, 485, 1977.
6. J. P. Bondorf, Proc. of EPS Topical Conf. on Large Amplitude Collective Nuclear Motions, Keszthely, Lake Balaton, Hungary, 10—16 June 1979 (KFKI Budapest 1979) Vol. II. p. 482.
4. L. P. Csernai, B. Lukács and J. Zimányi, Proc. Int. Workshop on Gross Properties of Nuclei and Nuclear Ecitations VII, Hirschegg, Kleinwalsertal, Austria, January 15—27 (1—79) Vol. A.; Ed. by H. Feldmeier (TH-Darmstadt, 1979) p. 133.
8. H. Gutbrod et al reported by M. Gyulassy in Proc. of EPS Topical Conf. on Large Amplitude Collective Nuclear Motions, Keszthely, Lake Balaton, Hungary, 10—16 June 1979, (KFKI, Budapest 1979) Vol. II, p. 601.
9. S. Nagamiya, L. A. Anderson, W. Brudener, O Chambarlain, M. C. Lemaire, S. Schnetzer, G. Shapiro, H. Steiner and I. Tahitata, Phys. Lett., *81B*, 147, 1979.
10. J. P. Blocki, J. Randrup, C. F. Tsang and W. J. Swiatecki, Ann. of Phys., *105*, 427, 1977.

Manuscript received by Akadémiai Kiadó: 29 March 1983
Manuscript received by the Printers: 20 April 1983
Date of publication: 29 October 1984

PRINTED IN HUNGARY
Akadémiai Kiadó és Nyomda, Budapest